Bulletin of Earth Sciences of Thailand

Remote sensing and mineral analysis of residual basalt from Khao Kradong area, Buriram, northeastern Thailand for jasmine rice growth experiment

Weerapon Kaew-in[1] and Montri Choowong[2*]

[1] Graduate School, Environmental Science, Chulalongkorn University, Bangkok 10330, Thailand
[2] Center of Excellence for the Morphology of Earth Surface and Advanced Geohazards in Southeast Asia (MESA CE), Department of Geology, Faculty of Science, Chulalongkorn University, Bangkok 10330 Thailand
* Corresponding author email: Montri.c@chula.ac.th

Received: 06 Jul 2023
Revised: 15 Aug 2023
Accepted: 18 Aug 2023

Abstract

Residual basaltic soil contains various primary, secondary, and micronutrients, including some unique plant characteristics such as the fragrance of rice. This paper shows the application of remote sensing coupled with X-Ray diffraction and X-Ray fluorescence analyses to locate the appropriate sites of residual basalt for the re-soil process of the jasmine rice growth experiment. We focused the geological investigation on the Khao Kradong Forest Park and the surrounding areas where an extinct volcano is located. The three series of satellite images taken in 2011, 2013, and 2021 were interpreted. As a result, we determined three target areas for excavating the residual soils. Fifty-four soil samples from seven profiles were analyzed by XRD and XRF. In conclusion, we found that the area with a distance of about 0.8 km far behind Huai Rat Sub-district Administrative Organization to the south, is the most suitable among all the basaltic residual soil sites that contain environmentally and chemically micronutrients appropriate to test the growth rate of jasmine rice.

Keywords: Residual basalt, Khao Kradong, Volcano, Buriram, Jasmine rice, Khao Dawk Mali 105 (KDML 105)

1 Introduction

Basalt, a common volcanic rock, often contains silicon in the form of silicon dioxide (SiO_2), also known as silica. The amount of silicon in basalt varies depending on the specific composition of the rock. In northeastern Thailand, basalt exposures are in the southern part of the Korat Plateau, Nakhon Ratchasima, Buriram, Surin, Sisaket, Ubon Ratchathani Provinces. The common and essential constituents of basaltic soil are SiO_2 45-55%, Al_2O_3 14%, CaO 10%, FeO 5-14%, MgO 5-12% TiO_2 0.5-2.0%, and total alkalis 2-6% reported by Department of Mineral Resources, Thailand between 2008-2013. The weathering process of silicon yields monosilicics acids (H_4SiO_4) and polysilicic acids that may affect plant growth and diseases. Monosilicis acid controls the chemical properties of the soil solution, and polysilicic acids affect the soil's physical

properties (Rodrigues and Datnoff, 2015). When plants absorb silicon from the soil, it can accumulate in the plant tissues, such as the leaves and stems. This accumulation can support the plant by strengthening cell walls and making them more resistant to pests, diseases, and environmental stresses, e.g., drought, high temperatures, and heavy metals (Imtiaz et al., 2016). Silica can also improve plant growth and yield by increasing photosynthesis, enhancing nutrient uptake, and promoting the production of enzymes and other compounds that help plants cope with stress (Eneji et al., 2008; Artyszak, 2018). It is worth noting that in addition to silicon, erosion, and weathering of basalt, pH, and soil nutrient levels create primary, secondary, and micronutrients, for example, aluminium, calcium, magnesium, iron, and potassium that are beneficial and, unique to plants such as fragrance (Singer et al., 1987; Choudhury et al., 2001; Bradbury et al., 2005; Changsri, 2015). Micronutrient from weathered basalt is essential for plant growth and development as well as for improving plant health and resilience. The number of micronutrients a plant requires can vary depending on the plant species, growing conditions, and other factors. Therefore, it is crucial to ensure that plants receive adequate amounts of those nutrients for optimal growth and performance.

In this work, we set up the objective to find the most suitable area among all the basaltic residual soil sites that contain environmentally and chemically micronutrients appropriate to test the growth rate of jasmine rice (Kamonwan et al., 2013). The field experiment will first be carried out at Udon Thani Province (see location in Fig. 1 top).

2 Material and methods

2.1 Remote sensing (RS) and Geographic Information System (GIS) of the study area

In this study, we focused on the Khao Kradong National Park and the surrounding areas where an extinct volcano is located (Fig. 1). We accessed various types of remote sensing (RS) data including (i) Thaichote (THEOS) satellite taken on February 10, 2013 (dry season) and corresponding to Zone 48N of the map projection, Universal Transverse Mercator (UTM) which uses the geodetic reference system WGS 1984, 4 multispectral. The resolution is 15 m for bands 1 to 4, respectively.

Blue (visible), Green (visible), Red (visible), and Near IR Landsat-5 TM satellite (Path 128 and Row 050) were taken on March 07, 2011 (dry season) and corresponding to Zone 48N of the map projection, UTM which uses the geodetic reference system WGS 1984. The resolution is 30 m for bands 1 to 5, respectively, including Blue (visible), Green (visible), Red (visible), Near IR, and SWIR. The resolution of band 6 is 120 m, and the resolution of band 7 is 30 m.

Finally, Landsat-8OLI satellite images (Path 128 and Row 050) were taken on June 22, 2021, corresponding to Zone 48N of the map projection, UTM which uses the geodetic reference system WGS 84. The resolution is 30 m for band OLI-1 to OLI-7 respectively: coastal/aerosol, Blue (visible), Green (visible),

Red (visible), NIR, SWIR-1, SWIR-2, and OLI-8 (Pan). The resolution is 15 m.

GIS data were applied to create the digital elevation model (DEM) derived from Landsat-8 OLI. Detail of GIS data including (i) Buriram province boundaries (province, district, sub-district), Polygon (reserved forest, water reservoir, wetland, and national park, basin), lines (stream, river, road), point (village, groundwater well). Geological GIS data include geological boundaries, aquifers, faults, soil groups, and land use and slope.

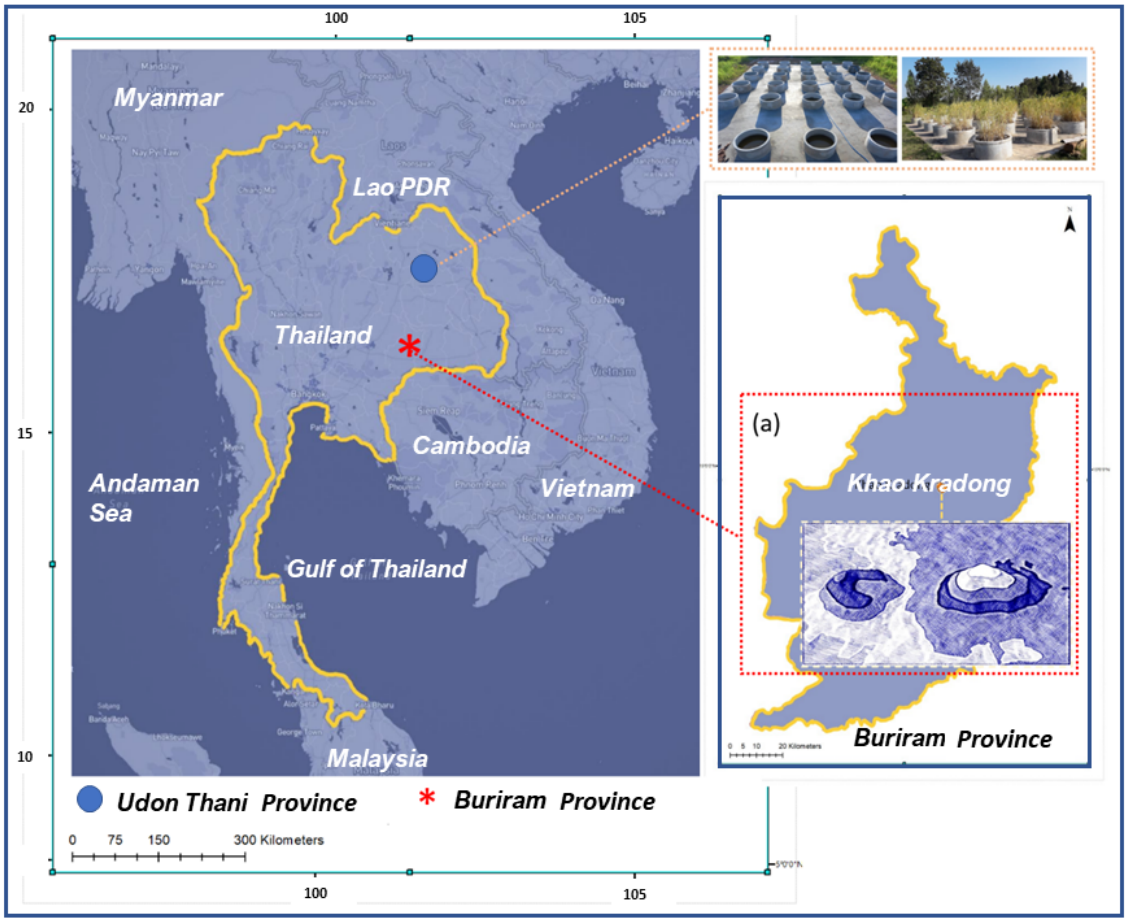

Figure 1 The map displays the locations of the residual basalt collection and the re-soil experiment site. (a) Residual basalt 3D map of Khao Kradong National Park, Buriram Province, northeastern Thailand. Photos on the top right show the re-soil and jasmine rice experimental area at Udon Thani Province.

2.2 RS and GIS analysis

Exploration of geological and obtaining comprehensive data are necessary for accurate information. However, only RS processing may not be enough. Therefore, we combined GIS and geospatial data of the study area including the DEM from Landsat-8OLI

satellite imagery. Satellite images from Thaichote (THEOS), Landsat-5TM, and Landsat-8OLI were classified using the maximum likelihood technique. The result is the distribution of basalt and residual basalt. All data was processed to define three target areas: 1, 2, and 3, to determine the storage location. The flowchart is shown in Figure 2.

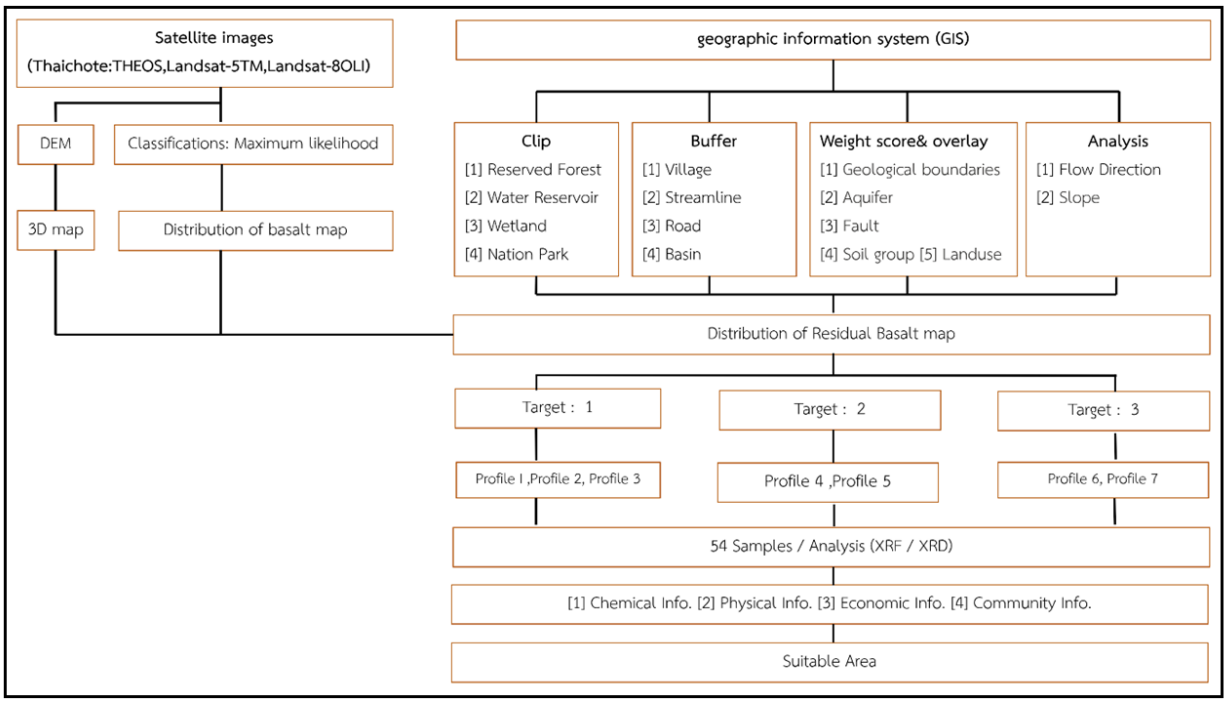

Figure 2 A flowchart shows GIS and RS data used in this study for the site selection process. Three series of satellite images were analyzed, especially to narrow down the distribution of basaltic soil as a GIS database map. The distribution of the residual basalt map was generated and divided into three target areas. Excavations were conducted to collect 54 soil samples for XRF and XRD analyses before locating the suitable area of residual soil quality for the jasmine rice experiment.

3 Results and Discussion

3.1 Distribution of residual basalt by RS and GIS

Three satellite images were processed, and the results showed the distribution of basalt in the study area. The 3D map is constructed to exhibit the physical features, consisting of two mountains, one resembling a crater. The hill on the west is slightly smaller than on the east side. The cavity is curved from the 3D map (also see Fig. 1a). We found that in this study, the Landsat-8OLI satellite image provided the most transparent distribution image, followed by the Thaichote and Landsat-5TM satellite images, respectively. Band 4 is vital for basalt classification. The distribution of basalt rock is distributed around Khao

Kradong in a wide area in all directions. But the density spread to the northeast of Khao Kradong, about 20 km from Muang Buri Ram District to Huai Rat District. The map is shown in Figure 3a. Fifty-four soil samples from seven profiles were analyzed by XRD and XRF (Fig. 3b).

The most suitable zone of residual basalt from this study is found from the Khao Kradong buffer zone 15 km of distance to the northeast (red cycle shown in Fig. 3b). The first target area is in Sawai Cheek Subdistrict, Muang Buriram District, about 4 km from the buffer zone. The second target area is the Huai Rat and Isan Subdistrict, 7 km from the buffer zone. The third target area is in Ban Yang Subdistrict, Mueang Buriram District, 12 km from the buffer zone. The three-target areas are shown in Figure 3b. After obtaining the target area, we created the profile point for the survey and sampling. Target area 1 contains three profiles (profiles 1, 2, and 3 in Fig. 3b). Target area 2 has two profiles (profiles 4 and 5). Target area 3 includes two profiles, profiles 6 and 7. The profile point is shown in Figure 3b.

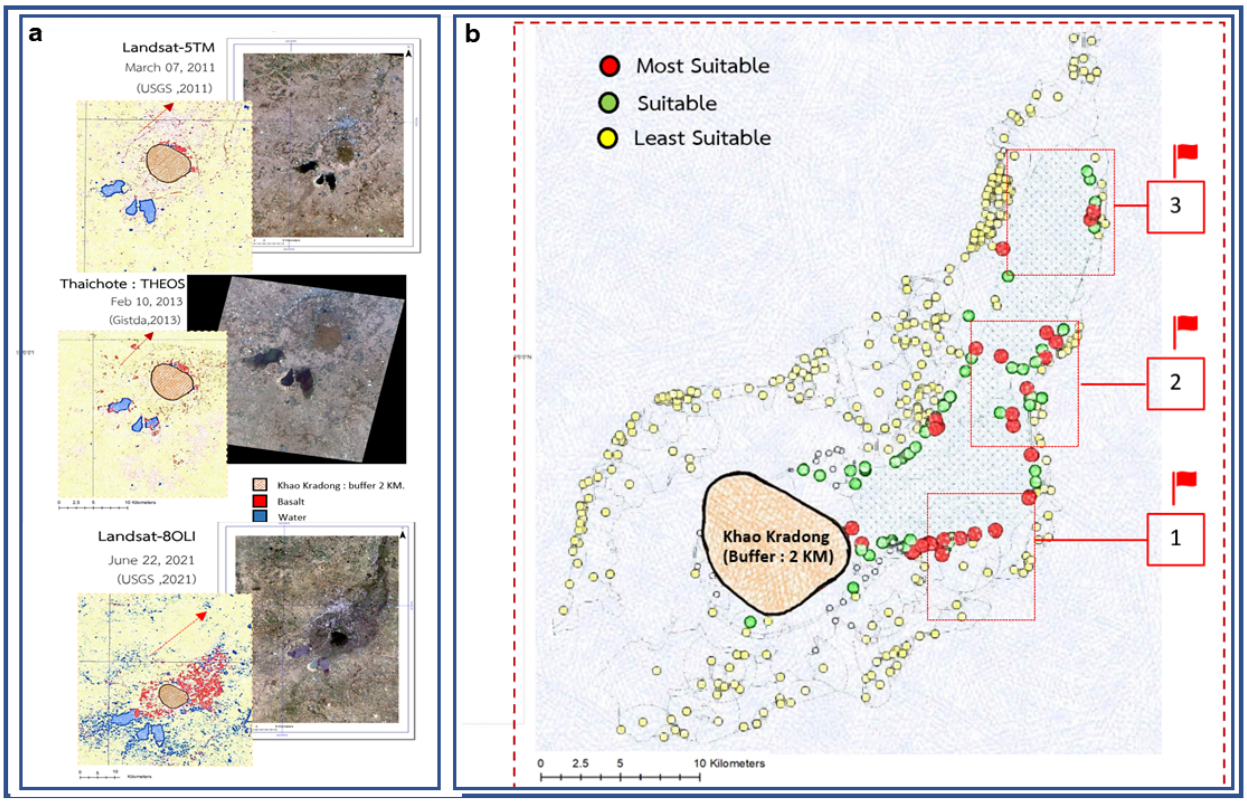

Figure 3 (a) Comparison of three satellite images. Landsat-8OLI satellite image (below) provides the most transparent distribution image, followed by the Thaichote (top) and Landsat-5TM (middle) satellite images, respectively. (b) Close-up of the distribution of sites from GIS and RS analyses, while three target areas (red circle dot) were identified.

3.2 Depth of residual basalt from coring

Originally, weathering basalt deposits were found as small sites between agricultural areas, such as a shallow basin and a rocky field. In the three-target areas, target area 1, profiles 1-3, depth 0-20 cm, we found the black and blown color of soil, mixed plant roots, soil ratio greater than rock, and sediment size. Coarse sand is recognized at depths 20-40 cm, gray-brown. The sediment size is fine sand with a depth of 40-60 cm, dark brown, sediment size is coarse sand, clay added more than 20-40 cm (clay: rock/60:40). At a depth of 60-70 cm, the mixed texture is the dark brown, proportion (clay: sand/80:20).

Target area 2, profiles 4 and 5, depth 0-20 cm, contains clay sediment and mixed rock in the ratio of 95: 5, dark brown-black color. There is mixed with coarse sand. At a depth of 20-40 cm, there is characterized by clay, and mixed rock in the ratio of 60:40, gray-brown color, and weathered rock. At a depth of 40-60 cm, the soil is mainly gray and has an orange color of weathered rock mixed with the ratio of clay: grain /40:60 with medium grain size. At a depth of 60-80 cm, the soil is light brown with a lot of weathered rocks. The ratio between clay and grain is 30:70 and found at depths between 80-110 cm. The soil is brown and orange. The ratio between clay per grain is 10:90 with grain size varying from coarse sand to pebbles. At depth 110-140 cm, mixed texture is found as dark red. The amount of soil is minimal. There are many rocks of various sizes. The ratio between soil and rock is 5:95 and found at a depth of 140-190 cm. The mixed texture is dark red with very little soil. There are many rocks of various sizes. The ratio between soil per rock is 3:97 with grain size ranging from 0.5 -3 mm.

In target area 3, profiles 6 and 7 with depth 0-20 cm, the mixed texture is dark brown with stone fragments. Clay per grain is 70:30 with grain size 0.1-2 cm of weathered basalt. At depth 20- 50 cm, mixed texture is composed of gray-brown and yellowish-brown. Clay per grain is 30:70 with a grain size of 0.5-3 cm. Some residual basalts are found. At a depth of 50-60 cm, mixed texture with weathered rock is recognized by yellowish brown, clay, and grey. Clay per grain is 40:60 with a grain size of 1-4 cm. Groundwater is found at depths of 60-70 m. Also, many rock fragments were found. The clay per grain ratio is 10: 90 with a grain size of 3-6 cm. The color and depth of the soil sample profile are shown in Figure 4(a).

In all seven profiles, the mixture ratio between soil and residual basalt at depths of 0-20 cm, 20-40 cm, 40-60 cm, 60-80 cm, 80-100 cm, and depths greater than 100 cm is 80: 20, 70: 30, 60: 40, 50: 50, 40: 60, and 30: 70,

respectively. The percentage of soil and residual basalt is shown in Figure 4(b). At depths greater than 100 cm, 2 mm or more rubble rocks were found in the mix, and the number of fragments increased with increasing depth. However, depth of 80 cm, the soil ratio is less than the amount of residual basalt. Therefore, it was unsuitable for agricultural cultivation because the aggregate of rock fragments is large (greater than 1 cm) mixed.

3.3 XRF and XRD

XRF analysis shows that silicon oxide (SiO_2) tends to increase with depth by concentration (%wt.) as follows. 50 % of silicon oxide is found at a depth of 0-20 cm, 51 % at depths of 20-60 cm, 54 % at depths of 60-100 cm, and 65 % at depths greater than 100 cm. Iron oxide (Fe_2O_3), aluminum oxide (Al_2O_3), titanium oxide (TiO_2), and potassium oxide (K_2O) decrease with increasing depth. At depths, 0-20 cm, iron, aluminum, titanium, and potassium oxide were 21%, 17%, and 5%, respectively. Depths at 20-60 cm, iron oxide, aluminum oxide, Ni oxide, and potassium oxide were found at 19%, 18%, and 5%, respectively. At a 60-100 cm depth, aluminum oxide, iron oxide, titanium oxide, and potassium oxide were found to be 17%, 15%, and 3%, respectively. The result of the XRF analysis is shown in Figure 4 (c).

From XRD analysis, the percentage of quartz increased with depth as follows; 56.84 % at a depth of 0-10 cm, 64.84% at a depth of 50-60 cm, and 80.64% at depths greater than 100-110 cm. Anorthoclase, montmorillonite, and ilmenite are unstable in each depth layer as follows. At depths of 0-10 cm, anorthoclase, montmorillonite, and ilmenite are found at 25.96 %, 10.21 %, and 6.48 %, respectively. At depth 50-60 cm, montmorillonite, albite, and ilmenite% are recognized as 22.89%, 7.81%, and 4.22%, respectively. At depths 100-110 cm, anorthoclase, and albite are found at 12.02%, 5.96%, and 0.71%, respectively. At a depth of 140-150 cm, Quartz, montmorillonite, calcite, and magnesian were found at 84.97%, 13.19%, and 1.01%, respectively. The result of the XRD analysis is shown in Figure 4(d).

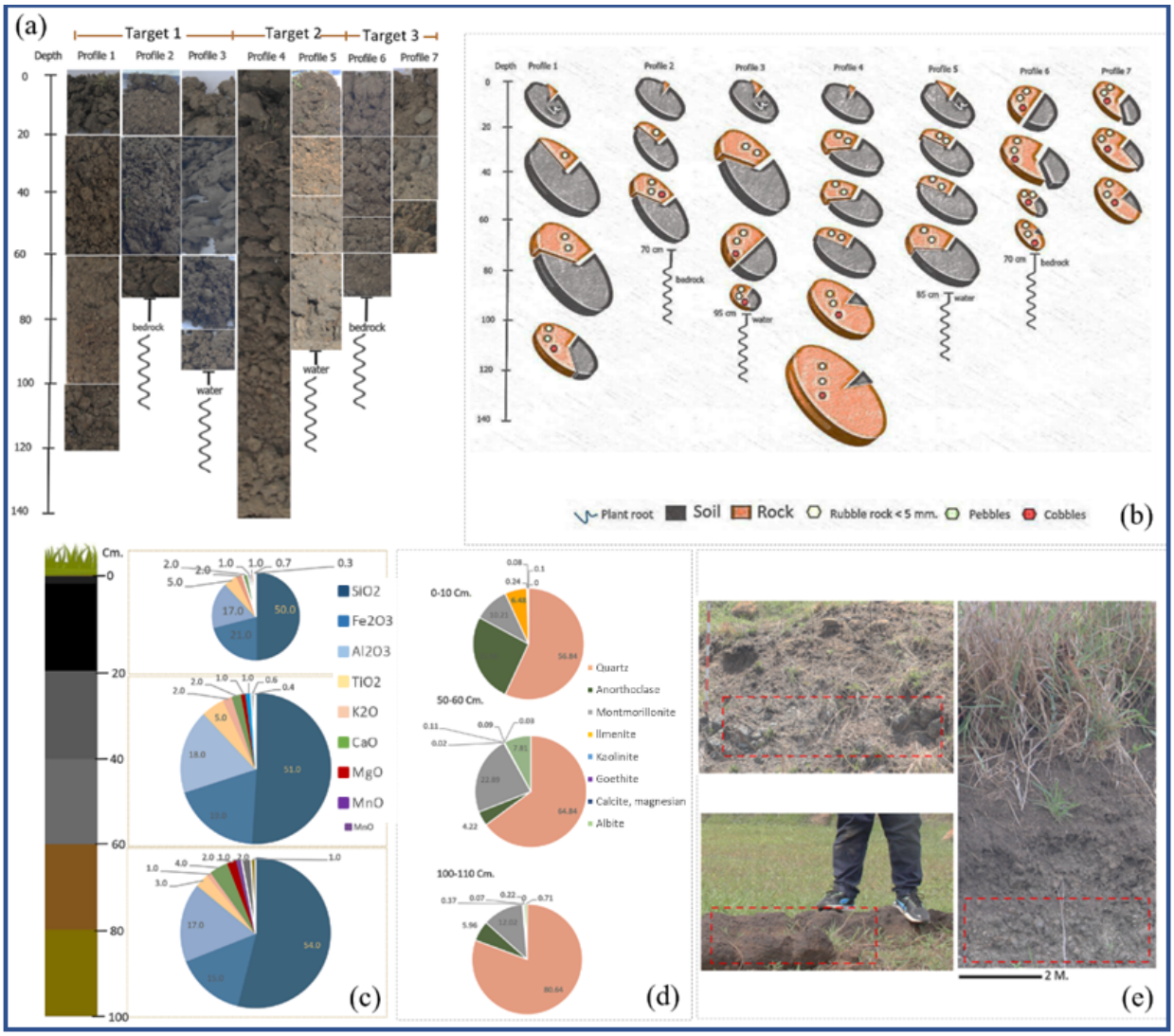

Figure 4 The result of coring, XRD, and XRF analysis. (a) The color and depth of the soil sample profile. (b) The percentage of soil and rock in the soil sample profile. (c) The result of XRF analysis. (d) The result of XRD analysis. (e) The traces and evidence of volcanic rocks in the study area.

4 Conclusion

This study concludes that the significant location of residual basalt was located at Muang Buriram District to Huai Rat District northeast of Khao Kradong. The area close to the Khao Kradong buffer zone (2 km) owns the most suitable target zone. Three target areas are located as far from the buffer zones as 4, 7, and 12 km. The high potential composition of residual basalt was found at a distance of 4 km (target 1) at a depth of 0-60 cm. At a depth of 0-80 cm, the soil texture is suitable for improving soil degradation or cultivation (Ndikuryayo et al., 2022). However, at depths greater than 80 cm, the amount of rock is more significant than the soil, including many small rock fragments, which is unsuitable for agricultural use. In terms of mineral composition, at depths from 20 cm onwards, more than 50% of SiO_2 was found, and the amount increased with increasing depth. At a depth of 50 cm, the quartz content was more than 60%, and the amount increased with increasing depth.

However, at some depths, the number of micronutrients is rather high. Nevertheless, the physical characteristics of the soil are not suitable for use in agriculture. We suggest that to select the location of the potential residual basalt in addition to physical and chemical data, it should also be considered together with the other information or context, such as information on the ease of accessibility of an area, consent, and cooperation from the landowner. Finally, here in this area, we suggest using residual basalt at a depth of 10-80 cm, a depth with mineral composition and soil texture appropriate for the re-soil experiment and for testing the growth rate of jasmine rice, especially the Khao Dawk Mali 105 (KDML 105).

Acknowledgments

The authors would like to thank IENS, Graduate School, and MESA CE of the Department of Geology, Chulalongkorn University, for all scholarship, resources, and laboratory support needed. The author would also like to thank the anonymous reviewers for their insightful comments that improved and all people who collaborated with this manuscript.

References

Artyszak, A. 2018. Effect of silicon fertilization on crop yield quantity and quality - a literature review in Europe. *Biochem*, 127, 152-160.

Bradbury, L. M. T., Fitzgerald, T. L., Henry, R. J., Jin, Q. & Waters D. L. E. 2005. The gene for fragrance in rice. *Plant Biotechnology Journal,* 3, 363-370.

Changsri, R. 2015. Factors affecting the quality of Thai Hom Mali Rice. *Rice Department Rice Research and Development Division*, Ubon Ratchathani Rice Research Center

Choudhury, P. R., Kohli, S., Srinivasan, K., Mohapatra, T. & Sharma, R. P. 2001. Identification and classification of aromatic rice based on DNA fingerprinting. *Euphotic,* 118, 243-251.

Eneji, A.E., Inanaga, S., Muranaka, S., Li, J., Hattori, T., An, P. & Tsuji, W. 2008. Growth and nutrient use in four grasses under drought stress as mediated by silicon fertilizers. *Journal of Plant Nutrition,* 31, 355-365.

Imtiaz, M., Rizwan, M. S., Mushtaq, M. A., Ashraf, M., Shahzad, S. M., Yousaf, B., Saeed, D. A., Rizwan, M., Nawaz, M. A., Mehmood, S. & Tu, S. 2016. Silicon occurrence, uptake, transport and mechanisms of heavy metals, minerals and salinity enhanced tolerance in plants with future prospects: A review. *Journal of Environmental Management*, 183, 521-529.

Kamonwan R., Srisawat k. & Sureeporn, K. 2013. Fragrance Gene and Molecular Basis of Fragrant Rice. *Thai Journal of Genetics* 6, 93-114.

Ndikuryayo C., Ndayiragije A., Kilasi N. & Kusolwa P. 2022 breeding for Rice Aroma and Drought Tolerance: *A Review Agronomy,* 12 (7).

Rodrigues F.A. & Datnoff L.E. (Eds) 2015. *Silicon and Plant Diseases*, Springer, Switzerland, 7-51.

Singer A. & Ben-Dor E. 1987. Origin of red clays layer interbedded with basalt of Golan Heights. *Geoderma,* 39, 293-306.